Journal of Microbiological Methods 243 (2026) 107429

Contents lists available at ScienceDirect

Journal of Microbiological Methods

journal homepage: www.elsevier.com/locate/jmicmeth

Determination of bacteria-specific odor signatures using low-cost metal oxide gas sensors

Emre Yavuzer [a,*], Mahmut Yılmaz [b]

[a] Department of Food Engineering, Faculty of Engineering, Niğde Ömer Halisdemir University, 51240 Niğde, Turkey
[b] Department of Food Engineering, Faculty of Agriculture, Kırşehir Ahi Evran University, 40100 Kırşehir, Turkey

ARTICLE INFO

Keywords:
Electronic nose
Volatile organic compounds (VOCs)
Time-derivative analysis (dVOC/dt)
Bacterial discrimination
Fish spoilage
Gas sensor array

ABSTRACT

In this study, a feasibility assessment was conducted to evaluate the potential of commercially available low-cost gas sensors for differentiating bacterial species inoculated into fish muscles. The signals were obtained by determining how low-cost gas sensors detected the volatile organic compound (VOC) patterns produced by each bacterial species (*Enterococcus faecalis, Pseudomonas luteola, Proteus mirabilis*, and *Photobacterium damselae*) in trout tissue. It was observed that MQ3 and MQ4 sensors yielded high rates for all bacteria, indicating a strong increase in broad VOC load consistent with the known cross-sensitivity range of MQ sensors as a result of bacterial metabolism. In addition to cumulative VOC patterns, time-dependent derivative analysis (dVOC/dt) was applied to reveal bacterium-specific metabolic differences in more detail. Thus, it was determined that *Photobacterium damselae*, unlike other bacteria, exhibited suppressed VOC production kinetics in the early stages, demonstrating that dynamic VOC fingerprints are a powerful tool for bacterial differentiation. The results demonstrate the feasibility of dynamic VOC fingerprinting using minimal sensor configurations for exploratory bacterial discrimination.

1. Introduction

Perishable fish and seafood-based foods play a significant role in the rise of microbial contamination-related deaths worldwide (Astuti et al., 2021; WHO, 2020). Accordingly, rapid and reliable detection of bacterial spoilage, especially in fishing, aquaculture, and processing stages, is vital for maintaining product safety and quality. In the process known as putrefaction, proteins and lipids are degraded by bacterial activity and volatile organic compounds (VOCs) are released (Kuley et al., 2019; Özoğul and Özoğul, 2000). Even with the most aseptic processing methods, it is impossible to restore the quality of a spoiled product using any technology. Therefore, modern food technology is working on rapid quality control systems that can detect changes in quality even when the product is still unspoiled and imperceptible to human senses. Electronic noses, biosensors, and machine learning methods are among the leading examples of these rapid quality control systems (de Oliveira et al., 2023; Henry et al., 2024; Jia et al., 2024; Saeed et al., 2022; Sharma et al., 2021; Xu et al., 2021; Yavuzer, 2023; Yavuzer and Köse, 2022).

Bacteria exhibit time-dependent VOC emission dynamics that can produce distinct sensor-response regimes during spoilage progression. The early stages of spoilage in food are often imperceptible to human senses. However, as the process progresses, the rapid (logarithmic) increase in bacterial activity leads to exceeding the defined acceptable limits for food safety.

This study aims to determine the digital fingerprint of different bacterial species on the same meat using MQ sensors. MQ sensors are easily accessible, compatible with open-source systems like Arduino, and capable of providing stable values. Previous studies have developed various models using these sensors for different plants, animals, food, and other industries (Chen et al., 2024; Fernández-Segovia et al., 2007; Huang et al., 2011; Rahimzadeh et al., 2019; Saeed et al., 2022; Wang et al., 2020; Yavuzer et al., 2025; Yavuzer et al., 2024). Although electronic nose systems are used for general spoilage detection in fish and food samples, most studies focus on general freshness classification rather than distinguishing specific spoilage or pathogenic bacteria within the same substrate. Furthermore, e-nose systems are expensive, limited to specific organizations, and rely on systems with limited reproducibility (due to restricted access to the equipment). Therefore, this study investigated the extent to which MQ sensors detect odors emitted by four different foodborne spoilage bacteria inoculated into fish meat, using a minimum sensor configuration to identify bacteria-specific volatile fingerprints.

* Corresponding author at: Department of Food Engineering, Faculty of Engineering, University of Niğde Ömer Halisdemir, 51240 Niğde, Turkey.
E-mail address: eyavuzer@ohu.edu.tr (E. Yavuzer).

https://doi.org/10.1016/j.mimet.2026.107429
Received 2 January 2026; Received in revised form 6 February 2026; Accepted 6 February 2026
Available online 7 February 2026

2. Material and methods

2.1. Sample preparation

Fresh fish meat (trout) was cut into 10 × 10 cm pieces. Each sample was prepared under sterile conditions, and 100 µL of inoculum suspension, standardized to a cell density of 10^8 cfu/mL, was applied to the surface of the fish meat using an automated pipette. The McFarland turbidity method was used to standardize bacterial inoculums to the 10^8 cfu/mL level. The test microorganisms used in the study were foodborne bacteria species *Enterococcus faecalis* (EF), *Pseudomonas luteola* (PL), *Proteus mirabilis* (PM), and *Photobacterium damselae* (PD), obtained from Çukurova University Department of Fisheries Engineering (Adana, Turkey). (Duan et al., 2024; Kuley and Özogul, 2011; Yavuzer and Kuley, 2020). Additionally, non-inoculated fish meat (CTRL) was included as a negative matrix control to account for endogenous background VOC emissions and to support normalization of sensor responses. Each bacterial condition was measured on one biological sample ($n = 1$). The e-nose setup and inoculated fish samples are illustrated in Fig. 1. All samples were kept at room temperature (25 °C) for 8 h. Ambient temperature and relative humidity were continuously monitored using an Arduino-based sensor module integrated into the measurement setup, and the environment was maintained at 25 ± 1 °C with relative humidity recorded within the 45–55% range throughout the experiment. Measurements were taken hourly from the sensors (MQ3, MQ4, MQ5, MQ8, MQ9, MQ135). This study was designed as an initial feasibility investigation to explore species-level separability of VOC response patterns using a minimal low-cost sensor array. Future work will include independent biological replicates to quantify intra-species variability and experimental repeatability under identical conditions.

2.2. Calculating AUC from sensor time series and generating species-specific VOC fingerprints

To quantitatively determine the volatile organic compound (VOC) release dynamics of four different bacterial species inoculated into fish meat, Area Under the Curve (AUC) values, representing the total VOC response over time, were calculated from sensor time series data.

2.3. Preparing sensor time series

Measurements for each bacterial species were obtained at 1-h intervals using sensors MQ3, MQ4, MQ5, MQ8, MQ9, and MQ135. Thus, a regular time series structure consisting of 8 time points was created for each sensor, ensuring the equal time step (Δt = 1 h) condition required for numerical integration. Since AUC calculation evaluates not only the magnitude of the signal but also its temporal continuity, it was able to more realistically represent the dynamic character of bacterial VOC production. AUC (Area **Under the Curve) Calculation:** For each sensor-bacteria pair, the total magnitude of VOC signals over time was calculated as follows:

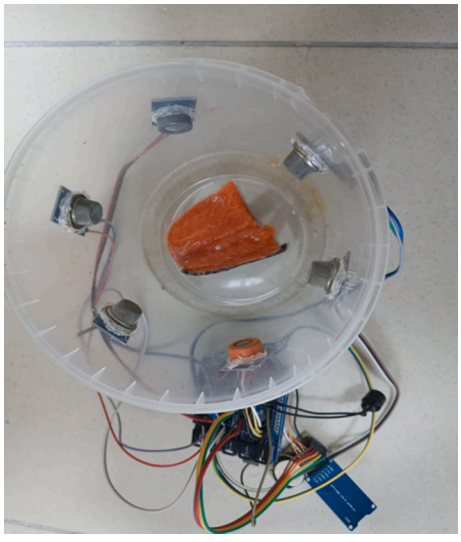

Fig. 1. Bacterial inoculated e nose environment (data represent single biological measurements, n = 1).

2.4. AUC

$$AUC_{b,i} = \sum_{t=1}^{N} S_{b,i}(t) \cdot \Delta t$$

Here.

$AUC_{b,i}$: Total VOC response of bacterium b at sensor i.

$S_{b,i}$ (t): Signal value of the relevant sensor at time t.

$N = 8$: Number of measurements (0–8 h).

Since the time steps are equal, the trapezoidal integration method was equivalent to the summing operation. Thus, individual AUC values reflecting bacterium-specific VOC production were obtained for each sensor.

2.5. Normalization based on blank sample

Raw AUC values include sensor sensitivity differences. Therefore, to reveal the true biological differences between bacterial species, all AUC values were normalized by ratioing them to a blank (control) sample in the same sensor. The normalization coefficient is defined as follows:

$$R_{b,i} = \frac{AUC_{b,i}}{AUC_{CTRL,i}}$$

This ratio is:

$R = 1.00 \rightarrow$ Bacteria did not produce VOC, same as Control.

$R > 1.00 \rightarrow$ Bacteria produced VOC, more than Control.

$R < 1.00 \rightarrow$ Bacteria generated a low response in the sensor (e.g., PD's negative fingerprint in MQ8).

It should be noted that $R < 1$ does not indicate the absence of VOC production, but rather reflects a sensor response lower than that of the non-inoculated matrix control. This may arise from limited sensor sensitivity to specific VOC classes or suppressed metabolic emission under the tested conditions.

These coefficients standardized and made comparable the VOC production power and sensor response profiles of bacterial species.

2.6. Creation of a species-specific VOC fingerprint matrix

The R_(b,i) values obtained by normalizing the AUCs for each bacterium created a six-dimensional VOC signature (VOC fingerprint) corresponding to six sensor axes. This matrix yielded the following:

1) Volatile compound profiles of each bacterium,
2) Sensitivity patterns of the sensors to VOC compound groups,
3) Metabolic differences between bacteria.

2.7. Time derivative (dVOC/dt) analysis

To evaluate the VOC production behavior of bacteria not only by their cumulative levels but also by their rate of change over time, the time derivative of the total VOC signal was calculated. Since measurements were obtained at equal time intervals (Δt = 1 h), the forward difference method was used in the derivative calculation. Numerical differentiation is inherently sensitive to noise; therefore, future studies may benefit from finer time resolution, smoothing/filtering strategies, and uncertainty estimation via independent biological replicates. Here, $S_{total}(t)$represents the overall normalized sensor response at time t.

$$\frac{dVOC}{dt}(t) = \frac{S_{total}(t+1) - S_{total}(t)}{\Delta t.}$$

This calculation determined the VOC rate-of-change values for each bacterial species at successive time intervals, making the response dynamics during early, mid, and late measurement intervals comparable. While AUC reflects cumulative VOC output, dVOC/dt provides complementary information about response kinetics and temporal VOC dynamics.

2.8. Data processing and visualization

Processing of raw sensor data, calculation of combined VOC signals, time derivative (dVOC/dt) analyses, and creation of tables and graphs were performed using MATLAB software (MathWorks Inc., Natick, MA, USA).

3. Results and discussion

In this study, a heat map was created to compare the total VOC production levels of four different bacterial species (EF, PL, PM, PD) on six different gas sensors (MQ3, MQ4, MQ5, MQ8, MQ9, MQ135) to a blank sample. This heat map is given in Fig. 2. The coefficients obtained by dividing the AUC values by the blank sample indicate the "VOC fingerprint" left by each bacterial species on each sensor. Because MQ sensors are cross-sensitive, interpretations are based on response-pattern differences rather than direct VOC identification.

The heat map showed that the MQ3 and MQ4 sensors, in particular, yielded high rates for all bacteria, indicating a strong increase in the overall VOC load as a result of bacterial activity, consistent with the broad cross-sensitivity profile of MQ sensors. The MQ8 sensor, however, produced a significantly lower response in the PD sample (0.36). This suggests that *Photobacterium damselae* exhibited a markedly suppressed response pattern on MQ8 compared with other bacteria, yielding a distinctive negative-like fingerprint for PD within the cross-sensor response profile.

Fig. 3 shows the VOC distributions of bacteria formed by plotting the normalized AUC values in six different MQ sensors in polar coordinates. From the radar graph, it was observed that EF, PL and PM species showed similarities in MQ3 and MQ4 sensors, but there were significant differences in the MQ8 and MQ9 regions.

Fig. 4 shows the VOC profiles of four bacteria on six sensors, reduced to two dimensions using Principal Component Analysis. PCA was used as an exploratory visualization tool to examine clustering tendencies among bacterial VOC profiles and does not represent supervised classification performance. The PC1 component explains 89.8% of the total

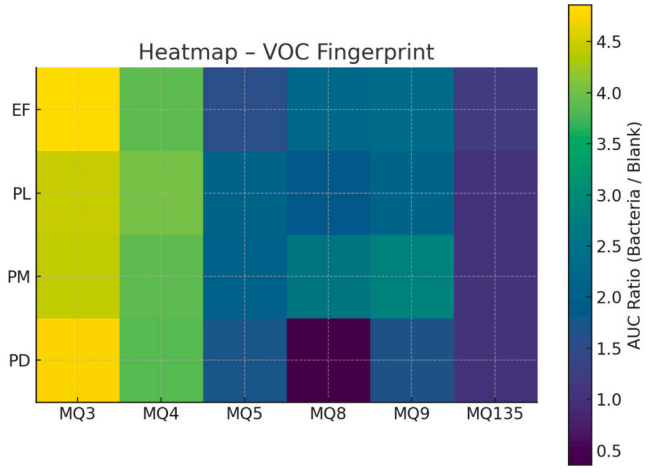

Fig. 2. Heat map obtained by dividing AUC values by Empty (data represent single biological measurements, n = 1).

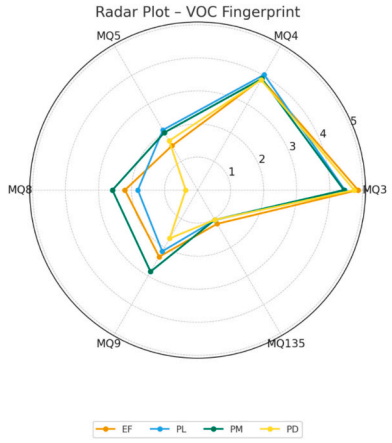

Fig. 3. Radar graph showing differences in VOC production among bacteria (data represent single biological measurements, n = 1).

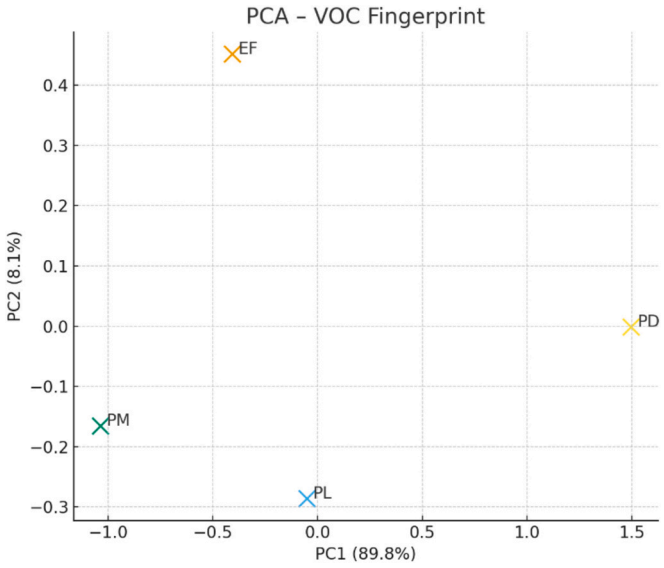

Fig. 4. PCA analysis based on VOC profiles (data represent single biological measurements, n = 1).

variance, while the PC2 component explains 8.1%. The data show that the VOC values are largely separated along a single axis, and they suggest a separation trend.

The graph shows that PD is clustered in a region far from all other species on the PC1 axis. The main reason for this separation is due to the extremely low VOC production of PD on the MQ8 sensor. However, PM and PL are positioned close to each other, EF shows a higher position on the PC2 axis, and MQ3 was able to form its own biological fingerprint due to its predominantly VOC production.

Fig. 5 shows the two-dimensional distribution of bacteria using the MQ3 and MQ8 sensors, which have the highest discrimination power in VOC fingerprint extraction. The data revealed that the two-sensor projection suggests an apparent separation trend, supporting the feasibility of minimal sensor configurations for exploratory discrimination. Although the EF, PL, and PM sensor values are close to each other on the MQ3 axis, the differences on the MQ8 axis highlight the differences in VOC production between species. The combination of these two sensors is inspiring for the design of a minimal biosensor system with its ability to offer high discrimination at low hardware cost.

The total VOC response produced by four bacteria applied to fish meat during a storage period of 0–8 h was evaluated using the AUC

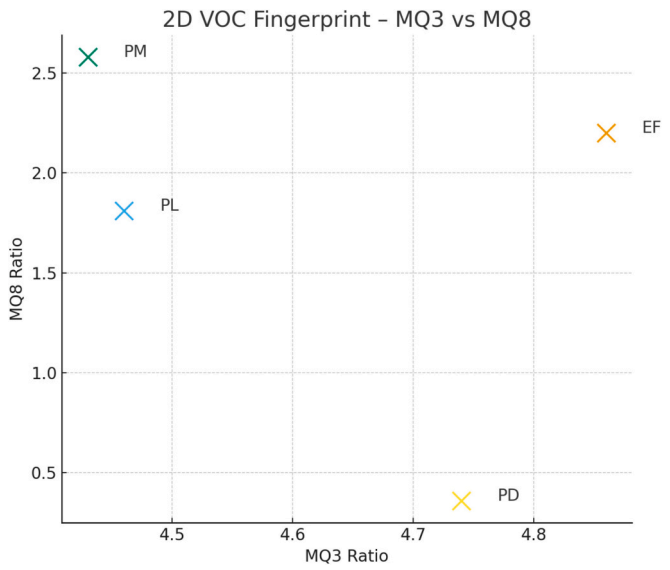

Fig. 5. Two-dimensional VOC fingerprint between MQ3 and MQ8 (data represent single biological measurements, n = 1).

values presented in Table 1. A very significant increase was observed in the MQ3 sensor for all bacteria compared to the blank sample. The increase in AUC values to the range of 4282–4640 in the EF, PL, PM, and PD groups indicates that bacterial activity rapidly increases mixed VOC emissions from the early measurement stages, reflected by elevated cross-sensitive MQ3 responses. This finding reveals that the MQ3 sensor acts as a "general VOC sensor" detecting the presence of bacteria and responds simultaneously to all types of contamination.

MQ4 sensor results showed that PL and PM species exhibited stronger MQ4 response patterns, consistent with increased emissions within VOC classes to which MQ4 is broadly sensitive. The fact that PL reached an MQ4 AUC of 3205 and PM reached 3030 suggests that these two species are particularly prominent in VOC response patterns that may reflect differences in substrate degradation dynamics. EF and PD showed a moderate increase in the MQ4 sensor.

In terms of the MQ5 sensor, the increase was more limited compared to MQ3 and MQ4, but bacterial contamination was still effectively detected. PL again reached the highest AUC value here, demonstrating its distinctive position in terms of an elevated MQ5 response profile within the overall VOC fingerprint. In contrast, PD's lower AUC in MQ5 compared to other species suggests that this species exhibited a lower MQ5 response magnitude compared with other bacteria within the measured VOC fingerprint.

The most significant species differentiation was observed in the MQ8 sensor. Table 1 shows that while the AUC values for EF, PL, and PM species ranged from 2671 to 3779, the MQ8 AUC value for PD was calculated as only 454. This difference clearly demonstrates that *Photobacterium damselae* exhibits a markedly reduced MQ8 response compared with the other species, forming a distinctive negative-like fingerprint on this sensor axis. In terms of AUC values, the MQ9 sensor differed from PL and PD with the high total VOC production of EF and PM reaching 2614. This indicates that EF and PM exhibited higher MQ9 response levels, suggesting differences in VOC emission patterns within classes broadly detectable by this sensor.

Table 2 presents the R values obtained by ratioing the AUC values to the control sample to eliminate scale differences arising from sensor performance. Table 2 is of great importance in revealing how the actual biological differences in VOC production are distributed among species. For example, the fact that all bacteria in the MQ3 sensor have an R value above 7 indicates bacteria produced approximately 7–8 times higher MQ3-normalized VOC response compared to the control group. This confirms that the MQ3 sensor functions as a strong biosensor in the early detection of contamination; however, it contributes little to species differentiation because the R values are close to each other. The R values of the MQ4 sensor similarly highlighted species differences. The $R = 4.83$ for PL and $R = 4.56$ for PM showed that these two species are metabolically more active in VOC classes broadly detectable by MQ4. The lower R values of EF and PD indicate that the MQ4 sensor is particularly more effective in differentiating Pseudomonas and Proteus species. In the MQ5 sensor, PL is seen to be distinguished from other species with an R value of 2.02. While this sensor is moderately effective in species differentiation, it provides a parameter that particularly supports the metabolic trace of PL. While PM and EF show moderate increases, the fact that PD produces the lowest R value indicates that this species presents a more limited profile in terms of VOC diversity compared to other species. The most striking species differentiation was observed in the R values of the MQ8 sensor, and the fact that PD produces only $R = 0.31$ in the MQ8 sensor shows that it produces VOCs far below even the control sample, and it has been determined to be a strong diagnostic biomarker.

The MQ9 sensor showed that EF and PM produced the highest R values ($R = 2.23$), while PL and PD had lower values. This result suggests that EF and PM exhibited stronger MQ9 response patterns, indicating differences in VOC emission profiles within gas classes broadly detectable by this sensor. In the MQ135 sensor, all species produced values very close to control ($R \approx 1.0$), showing that the total VOC load contributed only minimally to species differentiation. This result highlights that not all gas sensors with wide sensitivity contribute equally to bacterial differentiation, and that sensor selection, rather than the number of sensors, is crucial.

The values calculated by summing the average signal values obtained from the S < sub>total</sub>, MQ3, MQ4, MQ5, MQ8, MQ9, and MQ135 sensors for each time point are given in Table 3. The total VOC signals obtained from the combined sensor responses showed significant temporal differences among the four bacterial species. In the EF, PL, and PM species, the total VOC signal increased over time, but the rate and duration of the increase differed among the species.

Time derivative analysis (dVOC/dt) data are given in Table 4. The EF species showed a rapid early increase in VOC signal dynamics with high positive dVOC/dt values in the first 2–3 h of storage, followed by a gradual reduction in the VOC rate-of-change in later measurements. This pattern indicates an early rise in VOC signal behavior followed by stabilization in the rate-of-change profile. Because viable counts (CFU) were not measured in parallel, interpretations are limited to VOC signal dynamics and cannot directly confirm microbial growth phases. The PL species exhibited a fluctuating but overall high dVOC/dt profile,

Table 1
0–8 h AUC($\sum$S(t)) for each sensor and bacterium (each condition was measured on a single biological sample, $n = 1$).

Sensors	Empty	EF	PL	PM	PD
MQ3	587.41	4600.47	4493.27	4282.74	4640.67
MQ4	663.94	2485.93	3205.66	3030.47	3062.48
MQ5	1466.48	2543.06	2958.14	2667.33	2373.66
MQ8	1466.48	3459.66	2671.86	3779.99	454.28
MQ9	1172.80	2614.80	2215.60	2614.19	2010.40
MQ135	2248.46	2543.05	2419.88	2204.26	2135.07

Table 2
R values obtained by dividing the AUC values by the blank sample (each condition was measured on a single biological sample, n = 1).

Sensors	Empty	EF	PL	PM	PD
MQ3	1.00	7.83	7.65	7.29	7.90
MQ4	1.00	3.74	4.83	4.56	4.61
MQ5	1.00	1.73	2.02	1.82	1.62
MQ8	1.00	2.36	1.82	2.58	0.31
MQ9	1.00	2.23	1.89	2.23	1.71
MQ135	1.00	1.13	1.08	0.98	0.95

Table 3
Time-dependent total VOC signals of bacteria using a combined MQ sensor array (each condition was measured on a single biological sample, n = 1).

Time (Hours)	EF	PL	PM	PD
1	1821	1456	1279	1312
2	2011	1791	1781	1508
3	2129	1965	2185	1810
4	2266	2285	2396	1905
5	2436	2351	2663	2031
6	2329	2743	2726	2077
7	2421	2844	2806	2028
8	2494	2881	2748	2024

Table 4
Combined VOC production rate (dVOC/dt) (each condition was measured on a single biological sample, n = 1).

Time Interval	EF	PL	PM	PD
1–2	+190	+335	+502	+196
2–3	+118	+174	+404	+302
3–4	+137	+320	+211	+95
4–5	+170	+66	+267	+126
5–6	**−107**	**+392**	+63	**+46**
6–7	+92	+101	+80	**−49**
7–8	+73	+37	**−58**	**−4**

suggesting a response pattern that can sustain VOC production over time. The PM species showed the highest VOC rate-of-change values in the early period, followed by a decrease in dVOC/dt in later measurements, indicating a plateauing of the VOC kinetic response.

The results obtained for *Photobacterium damselae* (PD) differed significantly from other species. PD exhibited a limited rate of VOC signal increase in the early hours, while dVOC/dt values were close to zero or negative after the 5th hour. This indicates that PD not only has low total VOC response but also a suppressed VOC kinetic pattern during the measurement window.

The time-dependent variation of combined VOC production rates of bacteria is more clearly observed in Fig. 6. The results suggest that cumulative VOC metrics alone may not fully capture species-level separability, whereas time-derivative analysis (dVOC/dt) highlights differences in VOC emission kinetics more distinctly across bacterial conditions. In particular, the early saturation and negative dVOC/dt profile observed for PD show that this bacterium can be distinguished from other species with a dynamic biological fingerprint, and that electronic nose systems can be enhanced with time-sensitive analyses in early contamination detection. The experiment was conducted at 25 °C for 8 h to accelerate VOC evolution and enable feasibility evaluation within a practical measurement window. Future studies will investigate refrigerated storage, longer monitoring periods, and mixed microbial communities to better represent real-world spoilage conditions.

3.1. Limitations and future perspectives

This study represents an initial feasibility investigation based on single biological measurements and limited temporal resolution. The absence of independent biological replicates and parallel microbiological enumeration restricts quantitative interpretation of microbial growth kinetics. Furthermore, the cross-sensitivity of MQ sensors limits direct chemical attribution of VOC classes.

4. Conclusion

This study demonstrates that MQ-based electronic nose systems can be used to distinguish foodborne spoilage bacteria with low cost and high data throughput. The combined use of AUC-based fingerprinting and time derivative (dVOC/dt) analysis enabled the identification of bacteria-specific metabolic behaviors. *Photobacterium damselae* exhibited a distinct negative VOC fingerprint, particularly on the MQ8 sensor, showing that a minimum sensor configuration (MQ3–MQ8) suggests strong discrimination potential in an exploratory feasibility framework, offering a cost-effective and scalable model for monitoring early bacterial contamination in fish products.

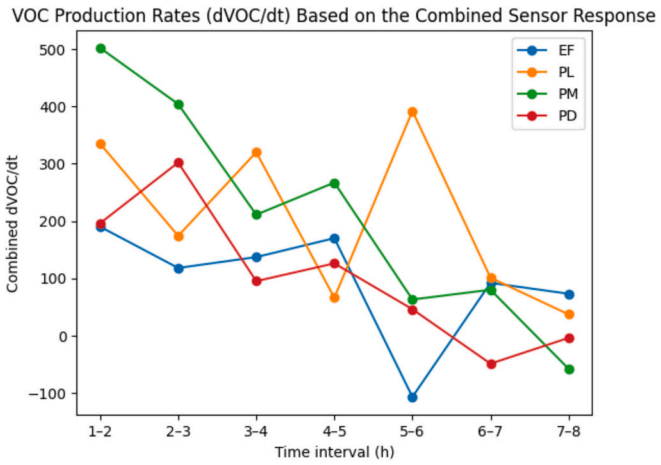

Fig. 6. VOC Production rates (dVOC/dt) based on the combined sensor response (data represent single biological measurements, n = 1).

Declaration of generative AI and AI-assisted technologies in the manuscript preparation process

During the preparation of this work the author(s) used ChatGPT in order to assist in refining the language, grammar, and scientific articulation in accordance with academic writing standards. After using this tool/service, the author(s) reviewed and edited the content as needed and take(s) full responsibility for the content of the published article.

CRediT authorship contribution statement

Emre Yavuzer: Writing – review & editing, Writing – original draft, Visualization, Validation, Supervision, Software, Resources, Project administration, Methodology, Investigation, Formal analysis, Data curation, Conceptualization. **Mahmut Yılmaz:** Validation, Resources, Methodology, Formal analysis.

Declaration of competing interest

The authors declare that they have no known competing financial interests or personal relationships that could have appeared to influence the work reported in this paper.

The author is an Editorial Board Member/Editor-in-Chief/Associate Editor/Guest Editor for this journal and was not involved in the editorial review or the decision to publish this article.

The authors declare the following financial interests/personal relationships which may be considered as potential competing interests:

Acknowledgement

This study is part of a PhD thesis in Agricultural Biotechnolgy at the Institute of Science, Kırşehir Ahi Evran University.

Data availability

Data will be made available on request.

References

Astuti, S.D., Tamimi, M.H., Pradhana, A.A.S., Alamsyah, K.A., Purnobasuki, H., Khasanah, M., Susilo, Y., Triyana, K., Kashif, M., Syahrom, A., 2021. Gas sensor array to classify the chicken meat with E. coli contaminant by using random forest and support vector machine. Biosens. Bioelectron.: X 9, 100083. https://doi.org/10.1016/J.BIOSX.2021.100083.

Chen, C.L., Liao, Y.C., Fang, M., 2024. Freshness evaluation of grouper fillets by inexpensive e-nose and spectroscopy sensors. Microchem. J. 198, 110145. https://doi.org/10.1016/J.MICROC.2024.110145.

de Oliveira, A.N., Bolognini, S.R.F., Navarro, L.C., Delafiori, J., Sales, G.M., de Oliveira, D.N., Catharino, R.R., 2023. Tomato classification using mass spectrometry-machine learning technique: a food safety-enhancing platform. Food Chem. 398, 133870. https://doi.org/10.1016/j.foodchem.2022.133870.

Duan, W.Y., Zhu, X.M., Zhang, S.B., Lv, Y.Y., Zhai, H.C., Wei, S., Ma, P.A., Hu, Y. Sen, 2024. Antifungal effects of carvacrol, the main volatile compound in Origanum vulgare L. essential oil, against aspergillus flavus in postharvest wheat. Int. J. Food Microbiol. 410, 110514. https://doi.org/10.1016/J.IJFOODMICRO.2023.110514.

Fernández-Segovia, I., Escriche, I., Fuentes, A., Serra, J.A., 2007. Microbial and sensory changes during refrigerated storage of desalted cod (Gadus morhua) preserved by combined methods. Int. J. Food Microbiol. 116 (1), 64–72. https://doi.org/10.1016/j.ijfoodmicro.2006.12.026.

Henry, J., Endres, J.L., Sadykov, M.R., Bayles, K.W., Svechkarev, D., 2024. Fast and accurate identification of pathogenic bacteria using excitation–emission spectroscopy and machine learning. Sens. Diagn. 3 (8), 1253–1262. https://doi.org/10.1039/D4SD00070F.

Huang, X., Xin, J., Zhao, J., 2011. A novel technique for rapid evaluation of fish freshness using colorimetric sensor array. J. Food Eng. 105 (4), 632–637. https://doi.org/10.1016/j.jfoodeng.2011.03.034.

Jia, Z., Luo, Y., Wang, D., Holliday, E., Sharma, A., Green, M.M., Roche, M.R., Thompson-Witrick, K., Flock, G., Pearlstein, A.J., Yu, H., Zhang, B., 2024. Surveillance of pathogenic bacteria on a food matrix using machine-learning-enabled paper chromogenic arrays. Biosens. Bioelectron. 248, 115999. https://doi.org/10.1016/J.BIOS.2024.115999.

Kuley, E., Özogul, F., 2011. Synergistic and antagonistic effect of lactic acid bacteria on tyramine production by food-borne pathogenic bacteria in tyrosine decarboxylase broth. Food Chem. 127 (3), 1163–1168. https://doi.org/10.1016/j.foodchem.2011.01.118.

Kuley, E., Yavuzer, M.N., Yavuzer, E., Durmuş, M., Yazgan, H., Gezginç, Y., Özogul, F., 2019. Inhibitory effects of safflower and bitter melon extracts on biogenic amine formation by fish spoilage bacteria and food borne pathogens. Food Biosci. 32, 100478. https://doi.org/10.1016/j.fbio.2019.100478.

Özoğul, F., Özoğul, Y., 2000. Comparison of methods used for determination of total volatile basic nitrogen (TVB-N) in rainbow trout (Oncorhynchus mykiss). Turk. J. Zool. 24 (1), 113–120.

Rahimzadeh, H., Sadeghi, M., Ghasemi-Varnamkhasti, M., Mireei, S.A., Tohidi, M., 2019. On the feasibility of metal oxide gas sensor based electronic nose software modification to characterize rice ageing during storage. J. Food Eng. 245, 1–10. https://doi.org/10.1016/J.JFOODENG.2018.10.001.

Saeed, R., Feng, H., Wang, X., Zhang, X., Fu, Z., 2022. Fish quality evaluation by sensor and machine learning: a mechanistic review. Food Control 137, 108902. https://doi.org/10.1016/j.foodcont.2022.108902.

Sharma, N., Sharma, R., Jindal, N., 2021. Machine learning and deep learning applications-a vision. Global Transitions Proc. 2 (1), 24–28. https://doi.org/10.1016/j.gltp.2021.01.004.

Wang, J., Chang, M., He, W., Lu, X., Fei, S., Lu, G., 2020. Withdrawn: optimization of electronic nose sensor array for tea aroma detecting based on correlation coefficient and cluster analysis. Sens. Actuators B, 128068. https://doi.org/10.1016/J.SNB.2020.128068.

WHO, 2020. No Title.

Xu, Y., Zhou, Y., Sekula, P., Ding, L., 2021. Machine learning in construction: from shallow to deep learning. Dev. Built Environ. 6 (February), 100045. https://doi.org/10.1016/j.dibe.2021.100045.

Yavuzer, E., 2023. Rapid detection of sea bass quality level with machine learning and electronic nose. Int. J. Food Sci. Technol. 58 (5), 2355–2359. https://doi.org/10.1111/IJFS.16365.

Yavuzer, E., Köse, M., 2022. Prediction of fish quality level with machine learning. Int. J. Food Sci. Technol. 57 (8), 5250–5255. https://doi.org/10.1111/ijfs.15853.

Yavuzer, E., Kuley, E., 2020. Testing the antimicrobial effects of some hydrosols on food borne-pathogens and spoilage bacteria. J. Limnol. Freshwater Fish. Res. 6 (1), 47–51. https://doi.org/10.17216/LIMNOFISH.618101.

Yavuzer, E., Yalçın, M.K., Uslu, H., Köse, M., 2024. Non-contact identification of essential oils with IR sensors and analysis of components with an electronic nose. Acta Aliment. 53 (3), 474–486. https://doi.org/10.1556/066.2024.00117.

Yavuzer, E., Yaprak Uslu, D., Köse, M., Yetişen, M., Alaşalvar, H., Şimşek, H.İ., 2025. Determination of quality levels of fish oils recovered from trout waste using machine learning and odor sensors. J. Food Meas. Charact. 1–10. https://doi.org/10.1007/S11694-025-03564-4/FIGURES/2.